

ARTICLE

Experimental Study on Ratio and Performance of Coal Gangue/Bottom Ash Geopolymer Double-Liquid Grouting Material

Wenqi Zhao¹, Wenbin Sun^{1,2,3,*}, Zhenbo Cao¹ and Jianbang Hao¹

¹College of Energy and Mining Engineering, Shandong University of Science and Technology, Qingdao, 266590, China

²State Key Laboratory of Coal Mining and Clean Utilization, China Coal Research Institute, Beijing, 100013, China

³College of Earth and Mineral Sciences, Pennsylvania State University—University Park, State College, PA 16801, USA

*Corresponding Author: Wenbin Sun. Email: swb@sdust.edu.cn

Received: 02 September 2022 Accepted: 09 November 2022 Published: 07 June 2023

ABSTRACT

Mine grouting reinforcement and water plugging projects often require large amounts of grouting materials. To reduce the carbon emission of grouting material production, improve the utilization of solid waste from mining enterprises, and meet the needs of mine reinforcement and seepage control, a double-liquid grouting material containing a high admixture of coal gangue powder/bottom ash geopolymer was studied. The setting time, fluidity, bleeding rate, and mechanical properties of grouting materials were studied through laboratory tests, and SEM analyzed the microstructure of the materials. The results show that the total mixture of calcined gangue does not exceed 60%. And the proportion of bottom ash replacing cement should be within 30%. At the same time, the volume mixture of sodium silicate is 20%. And the water-solid ratio does not exceed 0.6. The stability of the slurry prepared under this ratio is good. The microstructure of the stone body is dense, and its strength can meet the requirements of rock reinforcement and seepage control. Its economic and environmental benefits are more significant than the traditional cement-silicate double-liquid grouting material.

KEYWORDS

Coal gangue; municipal solid waste; sodium silicate; double liquid grouting material

1 Introduction

Coal resources are still the main energy in China, and there is still a huge consumption in the future for a long time. With the gradual reduction of shallow coal resources and the increasing depth of coal seam mining, under the effect of high stress and high water pressure, deep mining faces the problem of water inrush from mine aquifers, which usually requires grouting for rock reinforcement and seepage control of aquifers [1–3]. The commonly used grouting materials in the field of grouting reinforcement and anti-seepage are cement-based or cement-silicate double-liquid grouting materials [4]. However, in mine grouting projects, large-scale grouting imposes an economic burden on coal mining enterprises. At the same time, the production of cement materials consumes a large amount of energy. CO₂ emissions from its production process account for 5%–8% of global anthropogenic CO₂ emissions, which is inconsistent with the green development concept of global carbon emission reduction and carbon neutrality [5,6]. To address the environmental impact of mass production and the use of cement, scholars have been



developing supplementary cementitious materials as a partial replacement for cement to enhance material performance while reducing cement consumption [7,8]. Some scholars have also researched materials with high CO₂ absorption and reactivity from the perspective of their reactivity with CO₂ and applied them to the construction field to mitigate the greenhouse effect [9,10]. Meanwhile, some scholars have used waste materials to produce admixtures and added them to various cement products to change the performance of cement to meet various engineering requirements [11]. In the field of grouting materials and construction materials, using solid waste with extensive sources, low cost, low energy consumption, and low CO₂ emission instead of cement has become a hot research topic in recent years [12]. Zhang et al. used slag and fly ash to prepare an environmentally friendly grouting material with high strength, good flowability, low bleeding rate, and low porosity [13]. Zhang et al. prepared grouting materials with red mud and magnesium phosphate cement to reduce the use of cement and found that red mud improved the flowability of grouting materials, increased its strength, and reduced porosity [14]. Li et al. demonstrated experimentally the feasibility of producing high-strength mortar from seawater and coral sand [15]. Chu et al. prepared concrete blocks with strength comparable to that of using natural aggregates using recycled aggregates from construction solid waste [16].

With the further exploitation of mine resources, coal gangue has become the largest waste in coal production. Its spontaneous combustion and accumulation are extremely harmful to the environment, and the comprehensive utilization rate of coal gangue is not high for a long time. How to effectively utilize coal gangue is one of the important research directions of coal gangue treatment methods [17,18]. Li et al. used coal gangue and fly ash to prepare underground backfill material, which realized the comprehensive utilization of mine solid waste resources and solved the environmental problems caused by solid waste [19]. Yang et al. tested the effects of single and mixed activators on the setting time and strength of gangue-based geopolymers and concluded that mixed activators are more favorable to stimulating the hydration reaction of geopolymers [20]. According to XRD, TG-DTG, FT-IR, and SEM analysis, Yi et al. found that the hydration products of coal gangue geopolymer were mainly N-A-S-H gels and aluminosilicate zeolite crystals, which had a significant effect on the strength of the stone body [21]. Yan et al. analyzed the microstructure of metakaolin-sodium silicate double-liquid grouting material and found that the grouting material has good durability compared with ordinary cement-silicate double-liquid grouting material [22]. Guo et al. used coal gangue, fly ash, and slag to prepare grouting materials with clean production, high strength, and seepage pressure by response surface methodology [23]. Zhao et al. used uncalcined coal gangue and municipal solid waste incineration fly ash to prepare cementitious materials and found that the formation of N-A-S-H in the stone body provided strength, and the heavy metal ions in municipal solid waste incineration fly ash were solidified in the final formed geopolymer, reducing its toxicity [24].

With the acceleration of urbanization in China, the output of solid waste such as municipal waste is large and the utilization rate of resource utilization is low, which has caused a major obstacle to environmental protection. At present, the commonly used urban waste treatment method is mainly the landfill method, but the landfill method occupies a large area of land, which is easy to cause secondary pollution to the underground environment. In recent years, waste incineration technology has been gradually developed and applied, and the bottom ash remaining after incineration still has potential economic value, which is a research hotspot in the utilization of solid waste resources [25–29]. Li et al. and Yang et al. studied the feasibility of preparing blended cement from municipal solid waste incineration bottom ash, and the results showed that municipal solid waste incineration bottom ash has certain cementitious activity, but the cementitious activity is lower than that of cement, and the addition amount in cement should be controlled within 30% [30,31]. Zhang et al. analyzed the characteristics, modification treatment, and utilization of circulating fluidized bed combustion ash (CFBCA), which has pozzolanic activity and loose structure, and its f-CaO and SO₃ content lead to unstable material properties. CFBCA can be used as a

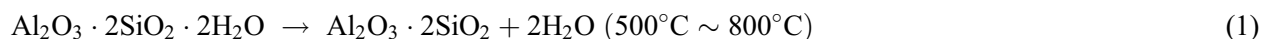
mineral admixture by modification treatment and as a low-carbon building material for making brick or synthesizing geopolymer [32]. Mohammad et al. summarized the material properties and engineering applications of coal bottom ash (CBA). CBA has high porosity and strong water absorption. The concrete prepared by CBA has good resistance to sulfate attack and dry shrinkage. It can be used as a substitute for cement in building materials and has good economic and environmental benefits [33].

Using coal gangue and municipal waste incineration bottom ash instead of cement to prepare grouting materials can improve the utilization rate of industrial solid waste and reduce carbon emissions during slurry production, thus protecting the mine and urban environment. In this paper, based on the principle of geopolymer reaction, on the basis of common cement-silicate double-liquid grouting material, we use activated coal gangue and municipal solid waste incineration bottom ash to replace part of the cement to prepare geopolymer double-liquid grouting material, and the solid waste is resourcefully utilized. The basic properties of the grouting material were studied through laboratory tests, and its economic and environmental benefits were compared with the traditional cement-silicate double-liquid grouting material to explore the possibility of preparing grouting materials with high admixture solid waste from mining enterprises.

2 Experimental Materials and Methods

2.1 Activation Mechanism of Coal Gangue

The main mineral components of coal gangue are kaolinite, montmorillonite, quartz sand, silicate minerals and carbonate minerals, among which the content of kaolinite can reach more than 60%. The raw material of coal gangue has almost no hydraulicity, and it needs to be activated by certain methods. The commonly used activation methods of coal gangue include thermal activation, mechanical activation, and chemical activation [34–36]. It has been mentioned in studies that kaolin clay is rich in aluminosilicate, and has a high reactivity when calcined at an intermediate temperature of 600°C–800°C [37,38]. The kaolinite crystal structure consists of silica-oxygen tetrahedral layer and aluminum-oxygen octahedral layer, each Al is connected with 2 O and 4 OH at the same time, under high-temperature calcination, the hydroxyl group is removed, and the coordination number of Al tends to 4 from 6, forming a poorly crystallized metakaolin, the atoms are irregularly arranged, showing a thermodynamically metastable state, and the ordered structure is transformed into a disordered system [39]. Similar to kaolin clay, when coal gangue is calcined, the binding water is removed and the crystal structure is destroyed, forming an amorphous metakaolin that produces large amounts of reactive Al₂O₃ and SiO₂, giving it volcanic ash activity. The specific chemical reaction equation of the coal gangue activation process is as follows [40,41]:



Through mechanical activation, that is, the effect of pulverization, the gangue particles can be refined, increasing their specific surface area. Under the effect of pulverizing, the crystal structure of aluminum-oxygen triangle and silica-oxygen tetrahedron within the gangue is destroyed and the degree of amorphous is increased, to improve the activity of gangue [42]. The Chemical activation method of coal gangue is mainly by adding an activator to participate in and accelerate the secondary reaction of coal gangue and cement hydration products. Under the action of alkaline substances, the covalent bonds of Si-O-Si and Al-O-Al in the material are broken, forming ions into the solution, and [SiO₄]⁴⁻ and [AlO₄]⁵⁻ in the solution combine to form a three-dimensional polymeric aluminate structure. With the occurrence of polymerization, the hydration products of a stable three-dimensional network structure are continuously generated, which improves the strength of the material. The polymerization mode can be expressed by the following general formula [43]:



M is alkali metal; m can be 1, 2, 3; n is polymerization degree; q is the amount of bound water.

The activation methods used in the preparation of coal gangue are usually not single. Generally, several activation methods are used simultaneously to obtain better material properties, namely, the composite activation method. In this paper, three methods of thermal activation, mechanical activation, and chemical activation are used to stimulate the activity of coal gangue. The coal gangue powder after calcination and grinding is selected, and sodium silicate is added as an alkali activator to prepare double-liquid grouting material.

2.2 Concept and Technology of Double Liquid Grouting

Double-liquid grouting is composed of two kinds of grouting slurry (liquid A, liquid B), which are stored in two containers, respectively. During the construction process, the two are pumped into the mixer together in a certain proportion through two pressure grout pumps and mixed, and quickly pumped out to the grout pipe for injection into the strata, its grouting process diagram as Fig. 1. The two solutions react rapidly to produce a gel substance that fills and gels the internal pores of the rock or soil, thus achieving the purpose of reinforcement and impermeability. Double-liquid grouting material has the advantages of short setting time, good stability, and not easy to lose, and is often used in foundation reinforcement and emergency plugging projects.

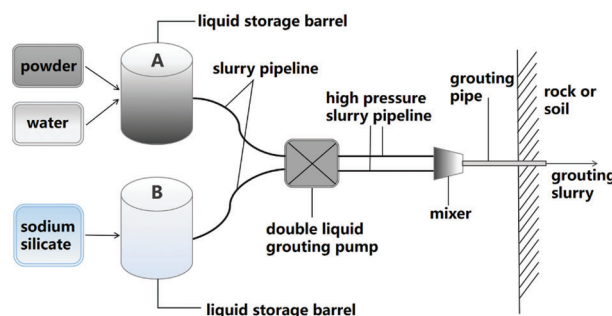


Figure 1: Schematic diagram of double-liquid grouting process

2.3 Selection of Materials

2.3.1 Calcined Coal Gangue

The 400 mesh calcined coal gangue powder produced in Hebei was selected and its chemical composition is shown in Table 1 and the particle size distribution is shown in Fig. 2.

Table 1: Chemical composition of the main component materials of grouting materials (%)

| Chemical composition | SiO ₂ | Al ₂ O ₃ | CaO | Fe ₂ O ₃ | MgO | K ₂ O | Na ₂ O | SO ₃ |
|---|------------------|--------------------------------|---------|--------------------------------|---------|------------------|-------------------|-----------------|
| Calcined coal gangue | 53~60 | 15~30 | 0.3~2.3 | 0.5~15 | 0.4~4 | 1~5 | 0.4~2.5 | — |
| Municipal solid waste incineration bottom ash | 45~52 | 6~13 | 20~39 | 4~8.4 | 1.2~3.2 | 1.3~2.9 | 0.6~3.3 | 0.5~3.9 |
| Cement | 19.66 | 6.39 | 61.67 | 3.66 | 3.01 | 0.95 | 0.3 | 3.02 |

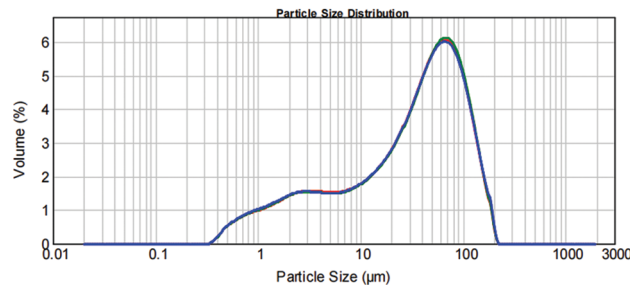


Figure 2: Particle size distribution of coal gangue powder

2.3.2 Municipal Solid Waste Incineration Bottom Ash

The municipal solid waste incineration bottom ash treated by screening, magnetic separation, and crushing is selected, and its composition is shown in Table 1. It can be seen from the table that the main chemical components of municipal solid waste incineration bottom ash are CaO and SiO₂, which are similar to the main chemical components of cement, and can be used instead of part of cement clinker in the experiment.

2.3.3 Cement

The PO425 Portland cement produced in Shandong is used, and its chemical composition is shown in Table 1.

2.3.4 Sodium Silicate

Using sodium silicate produced in Zhejiang area, modulus $m = 3.26$, Baume° Bé = 38.5.

2.3.5 Other Admixture

Polycarboxylate superplasticizer.

2.4 Test Material Ratio Design and Preparation Method

The orthogonal test has the characteristics of uniform dispersion, neatness, and comparability, and has high efficiency and economy in the multi-factor test. In this paper, the orthogonal test with four factors and three levels is used for the proportioning design of the slurry. Municipal solid waste incineration bottom ash is used as part of the substitute material of cement, and it is mixed with cement according to the test design proportion. The total content of calcined coal gangue powder in the cementitious material shall not be less than 50%. Based on the above materials, sodium silicate with different volume ratios is added as an alkali activator to prepare the double-liquid grouting material. Through the analysis and study of the water-solid ratio A, the proportion of solid waste incineration base ash instead of cement clinker B, the ratio of calcined coal gangue powder to total powder C, and the volume ratio of sodium silicate to geopolymer slurry D, the influence of these four factors on the performance of grouting materials is obtained, then the trend of the influence of each factor on the performance of the slurry is derived.

The design of the material composition distribution ratio of coal gangue/bottom ash geopolymer double-liquid grouting material is shown in Table 2. Among them, in order to make the grouting material have greater liquidity to ensure its injectability, while ensuring its later strength, adding polycarboxylate superplasticizer accounted for 2% of the quality of grouting powder.

Table 2: Composition design of experiment materials

| Group number | Factor A/ water- solid ratio | Factor B/proportion of solid waste incineration base ash instead of cement clinker% | Factor C/the ratio of calcined coal gangue powder to total powder% | Factor D/the volume ratio of sodium silicate to geopolymer slurry% |
|--------------|---------------------------------------|---|--|--|
| 1 | 0.4 | 10 | 50 | 20 |
| 2 | 0.4 | 20 | 60 | 40 |
| 3 | 0.4 | 30 | 70 | 60 |
| 4 | 0.6 | 10 | 60 | 60 |
| 5 | 0.6 | 20 | 70 | 20 |
| 6 | 0.6 | 30 | 50 | 40 |
| 7 | 0.8 | 10 | 70 | 40 |
| 8 | 0.8 | 20 | 50 | 60 |
| 9 | 0.8 | 30 | 60 | 20 |

The preparation process of slurry is as follows: according to the proportion shown in Table 2, the L9 (3⁴) orthogonal experiment table is selected, and a total of 9 groups of proportion experiments are carried out. Firstly, mix cement with calcined gangue powder and municipal solid waste incineration bottom ash according to the proportion, then add fixed proportion of water and polycarboxylate superplasticizer for mixing (liquid A), and finally add different volume ratio of sodium silicate (liquid B) and mix well.

2.5 Experimental Method

2.5.1 Fluidity Experiment

The fluidity of slurry was tested by the slurry fluidity test model. Firstly, put the glass plate in a horizontal position and wipe it with a damp cloth to make its surface wet, put the truncated cone round mold in the center of the glass plate and cover it with a damp cloth for later use. The material was stirred evenly according to the ratio and quickly poured into the truncated cone round mold. When the slurry and the top of the mold were flat, the pouring stopped and the mold was quickly lifted in the vertical direction. Because the sodium silicate double-liquid slurry setting time is fast, the maximum diameter of the two mutually perpendicular directions of the slurry flow part were measured based on the time point of the slurry solidification, and the average value was taken as the slurry fluidity.

2.5.2 Setting Time Experiment

Because the setting time of double-liquid slurry is short, usually within a few minutes, so the inverted cup method is used to test the setting time. Put the geopolymer slurry and the sodium silicate solution in two beakers respectively, pour them alternately in the two beakers and count the time until the slurry no longer flows.

2.5.3 Bleeding Rate Experiment

The grouting slurry is prepared according to the designed proportion and then poured into a 100 ml measuring cylinder, and then the measuring cylinder is sealed and placed in a flat position. Observe and record the volume of water separated from the slurry in the graduated cylinder every 10 min, and measure the water bleeding rate within 2 h. Bleeding rate = volume of precipitated water/100 × 100%.

2.5.4 Compressive Strength Experiment

Compressive strength tests were carried out on slurry concretions specimens with different curing periods. After coating the 70.7 mm × 70.7 mm × 70.7 mm mold with a layer of release agent and pouring in the proportionally configured slurry, scrape off the slurry that overflows the test mold part and vibrate it tightly. The specimens were placed in a curing box with a temperature of 20°C and relative humidity of 95% for 7 and 28-d, respectively, and the uniaxial compressive strength was tested. The experiment instrument is the electronic universal material testing machine. The loading speed is 0.1 kN/s. After the sample is damaged, the loading is stopped and the data is recorded.

The specific test procedure is shown in Fig. 3.

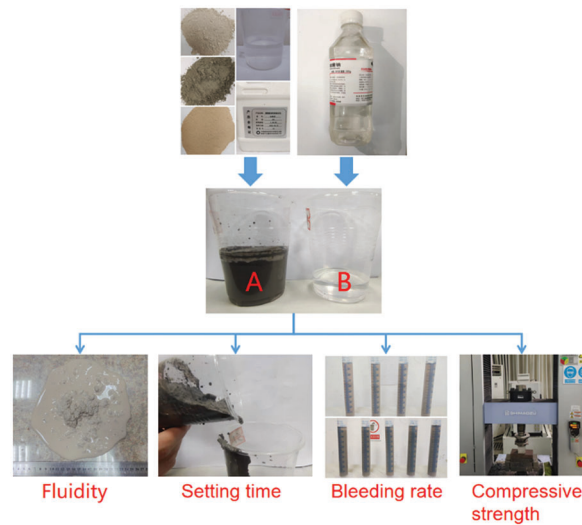


Figure 3: Test flow chart

3 Results and Analysis

3.1 Results of Orthogonal Experiment

The results of orthogonal experiment are shown in Table 3.

Table 3: Results of orthogonal experiment

| Group number | Fluidity/mm | Setting time/s | Compressive strength/MPa | | Bleeding rate/% |
|--------------|-------------|----------------|--------------------------|-------|-----------------|
| | | | 7-d | 28-d | |
| 1 | 65.0 | 10.05 | 7.49 | 11.21 | 0.06 |
| 2 | 66.0 | 14.11 | 5.32 | 6.94 | 0.06 |
| 3 | 80.5 | 19.95 | 0.19 | 2.16 | 0.08 |
| 4 | 185.5 | 135.36 | 0.14 | 2.07 | 0.11 |
| 5 | 98.5 | 14.78 | 2.35 | 5.25 | 0.13 |
| 6 | 190.0 | 26.56 | 2.20 | 5.12 | 0.15 |
| 7 | 200.0 | 105.38 | 0.10 | 1.83 | 0.33 |
| 8 | 148.0 | 10.88 | 0.13 | 2.05 | 0.35 |
| 9 | 193.0 | 22.36 | 1.70 | 3.76 | 0.37 |

3.2 Analysis of Setting Time

Setting time is one of the important factors to determine the performance of grouting material, which reflects the gelling speed of slurry, determines the pumpability, operability, and grouting diffusion range of slurry. A short setting time will cause blockage of the grouting pipe and a small diffusion range, while a long setting time will result in insufficient grouting reinforcement. The range analysis of experiments results is shown in Table 4, and the variation curves of setting time under all the factors are shown in Fig. 4.

Table 4: Range analysis of setting time

| Analysis item | Setting time/s | | | | Primary and secondary factors |
|---------------|----------------|-------|-------|-------|-------------------------------|
| | A | B | C | D | |
| K1 | 14.70 | 83.60 | 15.83 | 15.73 | B > A > C > D |
| K2 | 58.90 | 13.26 | 57.28 | 48.68 | |
| K3 | 42.21 | 22.96 | 46.70 | 55.40 | |
| R | 44.20 | 70.34 | 41.45 | 39.67 | |

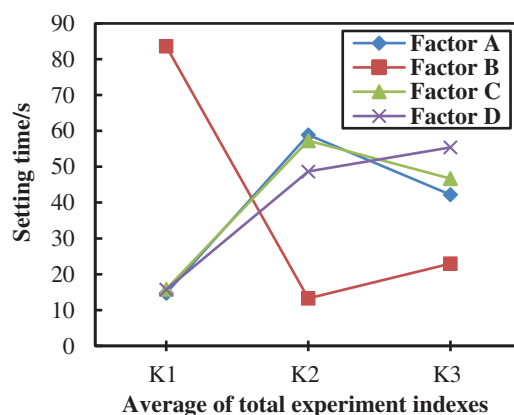


Figure 4: Curves of setting time under each factor

Combining the analysis of Table 4 and Fig. 4, the primary relationship among the four factors on the influence of slurry setting time of the grouting is B > A > C > D. With the increase in the content of calcined coal gangue, the setting time of the slurry shows an overall increasing trend. The reason is that the gel reaction in the early stage of the slurry is mainly carried out by the reaction of Ca(OH)₂ hydrolyzed by CaO in cement with sodium silicate to generate C-S-H gel. The increase in the content of calcined coal gangue reduces the CaO content in the slurry system and increases the time for the formation of the gel. The increase of sodium silicate content makes the slurry viscous, making it difficult to mix and react adequately, resulting in prolonged slurry setting time. The water-solid ratio rises, the spacing of solid particles in the slurry increases, its spatial flocculation structure forms slowly, and the overall slurry setting time tends to rise. When the water-solid ratio rises from K2 to K3, the overall viscosity of the slurry containing excess sodium silicate decreases at this point, making the reaction between liquid A and liquid B more adequate and the slurry setting time shortened to some extent. The content of incineration bottom ash at the K1 level is relatively small, so the effect on the setting time of the slurry is not significant. At this point, the main factor affecting the slurry setting time is the amount of coal gangue. The amount of incineration bottom ash added at the K2 level has a significant effect on the slurry setting time, which may be because of its fluffy powder, strong water absorption, accelerating the

slurry setting, while its high SO_3 content, and in the slurry system as SO_4^{2-} stimulates early hydration and reduces the setting time. When the substitution rate reaches 30%, because its CaO content is lower than cement, the Ca^{2+} content in the early hydration reaction is reduced, and the setting time is relatively longer.

3.3 Analysis of Fluidity

The fluidity of grouting slurry affects the pumpability and injectability of slurry, and to a certain extent determines the diffusion and filling performance of slurry in the grouting area, affecting the final effect of grouting. The slurry with appropriate fluidity can be prepared according to the diffusion range and reinforcement area required in practical engineering through fluidity research. The range analysis of the fluidity test results is shown in Table 5, and the fluidity change curve under each factor is shown in Fig. 5.

Table 5: Range analysis of fluidity

| Analysis item | Fluidity/mm | | | | Primary and secondary factors |
|---------------|-------------|--------|--------|--------|-------------------------------|
| | A | B | C | D | |
| K1 | 70.50 | 150.17 | 134.33 | 118.83 | A > B > D > C |
| K2 | 158.00 | 104.17 | 148.17 | 152.00 | |
| K3 | 180.33 | 154.50 | 126.33 | 138.00 | |
| R | 109.83 | 50.33 | 21.84 | 33.17 | |

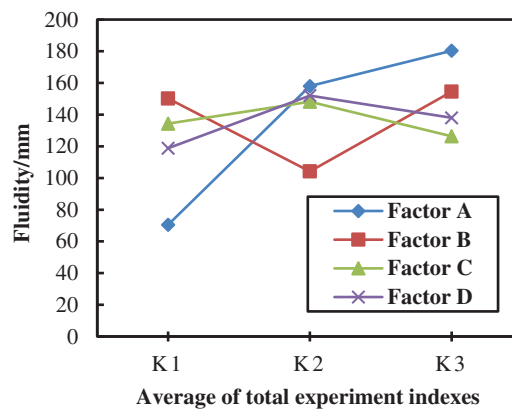


Figure 5: Curves of fluidity under each factor

Combining the analysis of Table 5 and Fig. 5, the primary relationship among the four factors on the influence of slurry fluidity of the grouting is A > B > D > C. With the increase of the water-solid ratio, the slurry becomes thinner and thinner, and the fluidity increases. When the addition of municipal solid waste is 20%, the effect of coal gangue/bottom ash geopolymers double-liquid grouting slurry fluidity changes abruptly, while the addition of 10% and 30% have the same effect on the slurry fluidity. When the addition amount of calcined coal gangue increases from 50% to 60%, due to the reduction of cement content in the slurry, the coagulation speed of the slurry becomes slower, which increases the fluidity in the early stage. When the addition amount of calcined coal gangue reaches 70%, due to the loose porous structure inside the coal gangue after calcination, the coal gangue has the ability to adsorb water during the slurry mixing, and its large addition reduces the fluidity. When the content of sodium silicate increases, the free water in the sodium silicate increases the water-solid ratio of the double-liquid grouting

slurry and the fluidity of the slurry increases. Therefore, the fluidity requirements of practical engineering can be met by properly adjusting the volume ratio of sodium silicate to liquid A.

3.4 Analysis of Bleeding Rate

The bleeding rate of the grouting slurry determines the stability of the slurry, which is particularly important in the process of long-distance transportation. If the bleeding rate of the grouting slurry is too large, the bleeding phenomenon will occur in the transportation process, and the slurry deposition will cause the blockage of the pipeline. Therefore, the bleeding rate test must be carried out to judge the stability of the slurry. The smaller the water bleeding rate, the better the slurry stability. Because the sodium silicate double-liquid grouting slurry has the characteristics of rapid setting, the mixed slurry will hardly separate water, and the double-liquid grouting slurry needs to be transported to the grouting area through two grouting pipelines in the grouting construction process and quickly combined with the reaction at the grouting mouth to form a stone body. Therefore, it is only necessary to test the influence of liquid A bleeding rate on storage and transportation. The range analysis of the bleeding rate test results is shown in Table 6, and the bleeding rate change curve under each factor is shown in Fig. 6.

Table 6: Range analysis of bleeding rate

| Analysis item | Bleeding rate/% | | | Primary and secondary factors |
|---------------|-----------------|------|------|-------------------------------|
| | A | B | C | |
| K1 | 0.07 | 0.17 | 0.19 | A > B > C |
| K2 | 0.13 | 0.18 | 0.18 | |
| K3 | 0.35 | 0.20 | 0.17 | |
| R | 0.28 | 0.03 | 0.02 | |

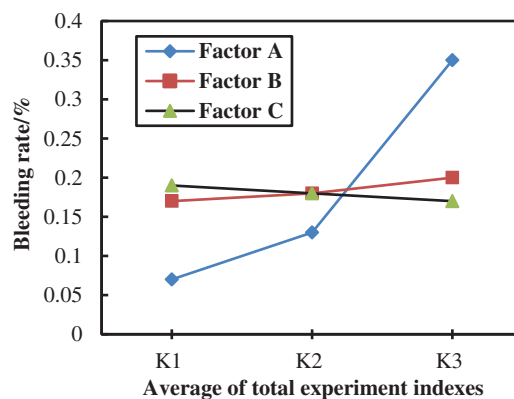


Figure 6: Curves of bleeding rate under each factor

Combining the analysis of Table 6 and Fig. 6, the bleeding rates of the slurry are all within 5%, indicating that the gangue-based solid waste slurry has good stability. The primary relationship among the four factors on the influence of the slurry bleeding rate of the grouting is A > B > C. The water-solid ratio is the main factor affecting the bleeding rate, and the liquid A bleeding rate of this double-liquid grouting material increases with the increase of the water-solid ratio. With the increase of the content of calcined coal gangue, the water bleeding rate of slurry decreases because of the strong adsorption of calcined coal

gangue to water, its high addition can make the slurry in a longer transport or storage time to maintain a low bleeding rate. Municipal solid waste incineration bottom ash will increase the bleeding rate of the slurry with the increase of the addition amount.

In the actual project, it is necessary to choose the appropriate water-solid ratio and powder proportion according to the slurry conveying distance or the complexity of the grouting area to ensure the stability of the slurry while having good fluidity and spreading distance.

3.5 Analysis of Uniaxial Compressive Strength

The strength of the grout stone body under external force is related to the stability and durability of the stone body after grouting. Especially in the deep mining of the mine, due to the influence of external force disturbance and high water pressure, the grouting material needs to have a certain strength to meet the needs of reinforcement and water plugging after solidification. The uniaxial compressive strength test was carried out on the specimens cured for 7 and 28-d under standard conditions. The range analysis of test results is shown in Table 7, and the compressive strength curve under each factor is shown in Figs. 7 and 8.

Table 7: Range analysis of uniaxial compressive strength

| Analysis item | Uniaxial compressive strength/MPa | | | | Primary and secondary factors | |
|----------------------|-----------------------------------|------|------|------|-------------------------------|---------------|
| | A | B | C | D | | |
| Curing period (7-d) | K1 | 4.33 | 2.57 | 3.27 | 3.84 | D > A > C > B |
| | K2 | 1.56 | 2.60 | 2.38 | 3.26 | |
| | K3 | 0.64 | 1.36 | 0.88 | 0.14 | |
| | R | 3.69 | 1.24 | 2.39 | 3.70 | |
| Curing period (28-d) | K1 | 6.77 | 5.03 | 6.12 | 6.74 | D > A > C > B |
| | K2 | 4.14 | 4.74 | 4.25 | 4.63 | |
| | K3 | 2.54 | 3.68 | 3.08 | 2.09 | |
| | R | 4.23 | 1.35 | 3.04 | 4.65 | |

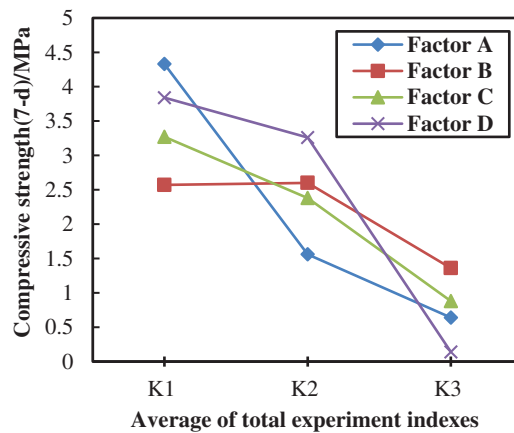


Figure 7: Curves of compressive strength (7-d) under each factor

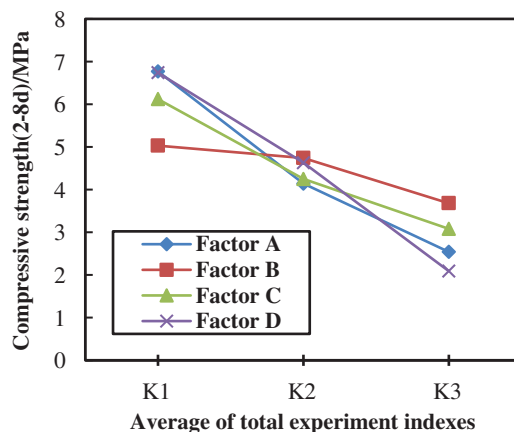


Figure 8: Curves of compressive strength (28-d) under each factor

Combining the analysis of Table 7, Figs. 7 and 8, The influence of each factor on the compressive strength of grout stone at 7 and 28-d is $D > A > C > B$. With the increase of sodium silicate addition, the compressive strength of the stone body showed a decreasing trend, and its different additions had a particularly obvious effect on the compressive strength of the stone body during the 7-d maintenance period. The addition of sodium silicate can improve the strength of the stone body in the short term. Still, its strength mainly comes from the gel generated by the hydration reaction with cement in the early stage. When the sodium silicate content is too much, it dilutes the slurry. At the same time, the excess sodium silicate that fails to react generates silica gel with too low strength, which decreases the stone body's overall strength. With the increase of calcined gangue and municipal solid waste content, the strength of the stone body shows a decreasing trend, and the decreasing trend is slower after 28-d. With the increase of the water-solid ratio, the strength of the stone body shows a decreasing trend, and the decreasing trend is more prominent when the water-solid ratio exceeds 0.6.

In summary, the volume ratio of sodium silicate in the double liquid grouting system should not exceed 20%. The excessive addition of sodium silicate will have a significant dilution effect on the slurry and reduce the strength of the stone body. The water-solid ratio should not exceed 0.6 and should be adjusted according to the needs of the actual project to meet the fluidity and compressive strength. To ensure the strength of the stone body, the addition of calcined coal gangue should not exceed 60%.

3.6 Microstructural Analysis

It can be seen from Fig. 9 that after the 28-d maintenance period, the slurry stone body containing 50% dose of calcined gangue and 20% volume dose of sodium silicate contains a large amount of fibrous C-S-H gel generated by early hydration. The hydrated sodium silica-aluminate gel (N-A-S-H) is generated by the active SiO_2 and Al_2O_3 in the late gangue powder with free Na^+ released from sodium silicate, both of which are interwoven and combined into a dense three-dimensional spatial network structure. And the mechanical properties of the stone body are better at this time. When the addition of calcined coal gangue reaches 70%, the concentration of Ca^{2+} in the slurry system decreases, the C-S-H produced by the early hydration reaction is less, the main product is N-A-S-H and mixed with more unreacted coal gangue pellets. At this time the internal structure of the stone body is loose, with more pores, and the corresponding strength is lower. When the volume admixture of sodium silicate is as high as 40%, the excessive sodium silicate dilutes the solid particles and hinders the further reaction of hydration products. Most hydration products are laminated C-H structures and coal gangue pellets with weak interlayer

connections and low strength. Calcined coal gangue and sodium silicate should be added in the appropriate range to ensure the stability of the strength of the stone body.

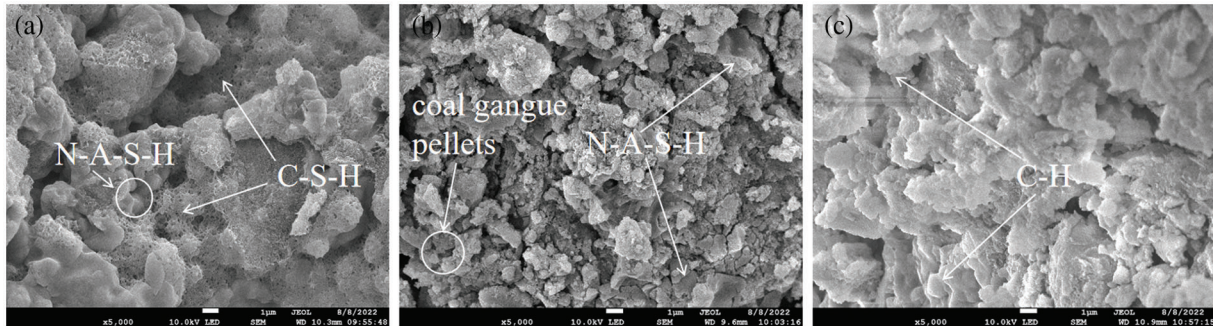


Figure 9: Microstructure of stone body (28 days curing period): (a) 50% calcined coal gangue and 20% sodium silicate; (b) 70% calcined coal gangue and 20% sodium silicate; (c) 50% calcined coal gangue and 40% sodium silicate

3.7 Applicability Analysis of Coal Gangue/Bottom Ash Geopolymer Double-Liquid Grouting Material

3.7.1 Water Plugging Performance Analysis of Grouting Material

According to the reference [44], the reinforced impermeable material needs a certain shear strength to prevent the slurry stone body from being squeezed out of the fissure by water pressure, so as to resist the seepage failure of high water pressure. This performance can be checked with the Buckingham-Reiner formula:

$$\tau_s = \frac{PB}{2b} \quad (3)$$

In the formula: τ_s -shear strength, MPa; P-permeability pressure of groundwater, MPa; B-gap width, mm; b-curtain thickness, mm.

Assuming that the groundwater in the grouting area has a high water pressure of 4 MPa, the crack width is 10–20 mm, and the curtain thickness is 1000 mm, the shear strength required to destroy the grouting grout stone body can be obtained from the formula (3) to be 0.04 MPa. The tensile strength of the stone body is generally 1/20–1/10 of the compressive strength, and the shear strength is located between them. The 1/20 of the compressive strength of the stone body is taken as the shear strength. The minimum compressive strength obtained in this paper's 28-d curing period of the stone body specimen is 1.83 MPa, and its shear strength of 0.09 MPa also exceeds the shear strength required for failure. Therefore, coal gangue/bottom ash geopolymer double-liquid grouting material can be used as an anti-seepage material to resist high water head damage.

3.7.2 Analysis of the Economic and Environmental Benefits and Performance of Grouting Materials

Combined with the analysis of Tables 3 and 8, although the stone body strength of coal gangue/bottom ash geopolymer double-liquid grouting material is lower than that of traditional cement-silicate double-grouting material, its later strength increases significantly. When the addition amount of calcined coal gangue reaches 60% or the addition amount of municipal solid waste incineration bottom ash reaches 20% (The volume addition of sodium silicate is kept at 20%~40%), its strength still meets the basic engineering needs. Compared with ordinary cement-sodium silicate slurry, the manufacturing cost of coal gangue/bottom ash geopolymer double-liquid grouting material is lower, and its CO₂ emission in the production process is greatly reduced [45]. The calcination temperature of coal gangue is much lower than the production temperature of cement clinker, and the energy consumption is lower.

Table 8: Analysis of the economic and environmental benefits and performance of grouting materials

| Grouting material | Cement-silicate double-grouting material | Coal gangue/bottom ash geopolymer double-liquid grouting material |
|--|--|---|
| 7-d compressive strength/MPa | 12.2 | 7.49 |
| 28-d compressive strength/MPa | 15.7 | 11.21 |
| Strength growth rate | 28.7% | 49.6% |
| CO ₂ emissions per ton of material produced/t | 1.38 | 0.28 |
| Temperature required for material production | 1400°C~1450°C | 500°C~750°C |
| Cost/(¥/t) | 450~500 | 380~400 |

To summarize the above, the wide source and low price of solid waste materials significantly reduce the cost of grouting for underground projects, while the reduced amount of cement reduces the amount of non-renewable energy used to produce cement and the amount of CO₂ emissions. The geopolymer double-liquid grouting material has the characteristics of a fast setting, the later strength increases greatly, and the internal three-dimensional network structure of the stone body by C-S-H and N-A-S-H interwoven combination is more stable, overcoming the shortcomings of single-liquid cement grouting material with long setting time and easy leakage after grouting and common cement-silicate double-liquid grouting material that is easily eroded by water and poor durability. Therefore, geopolymer double-liquid grouting material is more suitable for underground rock and soil filling, reinforcement, and isolation waterproof plugging projects in a water-rich environment.

4 Conclusions

Deep mine reinforcement and anti-seepage double-liquid grouting materials were prepared using solid waste. The ratio and performance of coal gangue/bottom ash geopolymer double-liquid grouting material were studied through laboratory tests and microscopic analysis. The performance and economic and environmental benefits were compared with those of traditional cement-silicate double-liquid grouting material. The following conclusions are drawn:

1. Under the combined action of three activation methods of calcination, grinding, and adding a chemical activator, adding calcined coal gangue in the range of 50% to 60% can prepare grouting materials that meet the needs of deep mine reinforcement and anti-seepage, which improves the utilization rate of coal gangue.
2. The orthogonal test shows that the municipal solid waste incineration bottom ash has a certain cementitious activity, and the impact on the compressive strength performance of the double-liquid grouting system is stable at a replacement rate of less than 30%.
3. The range analysis of orthogonal test shows that in the coal gangue/bottom ash geopolymer double-liquid grouting material system, the water-solid ratio and the addition amount of municipal solid waste incineration bottom ash have obvious influences on the setting time, fluidity and bleeding rate of the slurry. The addition of sodium silicate and water-solid ratio play a major role in controlling the compressive strength of slurry stones. Sodium silicate volume admixture in 20% is the best, and the water-solid ratio should not exceed 0.6.

4. The coal gangue/bottom ash geopolymer double-liquid grouting material meets the reinforcement and seepage control requirements of deep mines and is economically superior. Its carbon emission in the production process is much lower than traditional cement-silicate double-liquid grouting material, which is conducive to the protection and improvement of the ecological environment of mines and cities.

Funding Statement: The research described in this paper was financially supported by the National Natural Science Foundation of China (No. 51974172), Innovation and Technology Program of Universities in Shandong Province, China (No. 2020KJH001), National Natural Science Foundation of China (No. 52274131), State Key Laboratory of Coal Mining and Clean Utilization (No. 2021-CMCU-KF017).

Conflicts of Interest: The authors declare that they have no conflicts of interest to report regarding the present study.

References

1. Sun, W., Xue, Y., Li, T., Liu, W. (2019). Multi-field coupling of water inrush channel formation in a deep mine with a buried fault. *Mine Water and the Environment*, 38(3), 528–535. <https://doi.org/10.1007/s10230-019-00616-2>
2. Zhou, F., Sun, W., Shao, J., Kong, L., Geng, X. (2020). Experimental study on nano silica modified cement base grouting reinforcement materials. *Geomechanics and Engineering*, 20(1), 67–73. <https://doi.org/10.12989/gae.2020.20.1.067>
3. Zhao, J. H., Liu, Q., Jiang, C. B., Wang, D. F. (2022). Application of rock mass index in the prediction of mine water inrush and grouting quantity. *Geomechanics and Engineering*, 30(6), 503–515. <https://doi.org/10.12989/gae.2022.30.6.503>
4. He, S., Lai, J., Wang, L., Wang, K. (2020). A literature review on properties and applications of grouts for shield tunnel. *Construction and Building Materials*, 239, 117782. <https://doi.org/10.1016/j.conbuildmat.2019.117782>
5. Tosti, L., van Zomeren, A., Pels, J. R., Damgaard, A., Comans, R. N. J. (2020). Life cycle assessment of the reuse of fly ash from biomass combustion as secondary cementitious material in cement products. *Journal of Cleaner Production*, 245, 118937. <https://doi.org/10.1016/j.jclepro.2019.118937>
6. Miller, S. A., Myers, R. J. (2020). Environmental impacts of alternative cement binders. *Environmental Science & Technology*, 54(2), 677–686. <https://doi.org/10.1021/acs.est.9b05550>
7. Chu, S. H. (2019). Effect of paste volume on fresh and hardened properties of concrete. *Construction and Building Materials*, 218, 284–294. <https://doi.org/10.1016/j.conbuildmat.2019.05.131>
8. Chu, S. H., Kwan, A. K. H. (2019). Co-addition of metakaolin and silica fume in mortar: Effects and advantages. *Construction and Building Materials*, 197, 716–724. <https://doi.org/10.1016/j.conbuildmat.2018.11.244>
9. Chen, Z. X., Chu, S. H., Lee, Y. S., Lee, H. S. (2020). Coupling effect of γ -dicalcium silicate and slag on carbonation resistance of low carbon materials. *Journal of Cleaner Production*, 262, 121385. <https://doi.org/10.1016/j.jclepro.2020.121385>
10. Chen, Z. X., Chu, S. H., Ishak, S., Lee, H. S., Zhao, Q. X. et al. (2022). Roles of particle packing and water coating thickness in carbonation and strength of γ -dicalcium silicate-based low carbon materials. *Journal of Cleaner Production*, 358, 131735. <https://doi.org/10.1016/j.jclepro.2022.131735>
11. Dong, H., Unluer, C., Yang, E. H., Al-Tabbaa, A. (2018). Recovery of reactive MgO from reject brine via the addition of NaOH. *Desalination*, 429, 88–95. <https://doi.org/10.1016/j.desal.2017.12.021>
12. Luukkonen, T., Abdollahnejad, Z., Yliniemi, J., Kinnunen, P., Illikainen, M. (2018). One-part alkali-activated materials: A review. *Cement and Concrete Research*, 103, 21–34. <https://doi.org/10.1016/j.cemconres.2017.10.001>
13. Zhang, Z., Tian, Z., Zhang, K., Tang, X., Luo, Y. (2021). Preparation and characterization of the greener alkali-activated grouting materials based on multi-index optimization. *Construction and Building Materials*, 269, 121328. <https://doi.org/10.1016/j.conbuildmat.2020.121328>

14. Zhang, J., Li, S., Li, Z., Liu, C., Gao, Y. et al. (2020). Properties of red mud blended with magnesium phosphate cement paste: Feasibility of grouting material preparation. *Construction and Building Materials*, 260, 119704. <https://doi.org/10.1016/j.conbuildmat.2020.119704>
15. Li, L. G., Xiao, B. F., Fang, Z. Q., Xiong, Z., Chu, S. H. et al. (2021). Feasibility of glass/basalt fiber reinforced seawater coral sand mortar for 3D printing. *Additive Manufacturing*, 37, 101684. <https://doi.org/10.1016/j.addma.2020.101684>
16. Chu, S. H., Poon, C. S., Lam, C. S., Li, L. (2021). Effect of natural and recycled aggregate packing on properties of concrete blocks. *Construction and Building Materials*, 278, 122247. <https://doi.org/10.1016/j.conbuildmat.2021.122247>
17. Ren, B., Zhao, Y., Bai, H., Kang, S., Zhang, T. et al. (2021). Eco-friendly geopolymer prepared from solid wastes: A critical review. *Chemosphere*, 267. <https://doi.org/10.1016/j.chemosphere.2020.128900>
18. Li, J., Wang, J. (2019). Comprehensive utilization and environmental risks of coal gangue: A review. *Journal of Cleaner Production*, 239, 117946. <https://doi.org/10.1016/j.jclepro.2019.117946>
19. Li, M., Zhang, J., Li, A., Zhou, N. (2020). Reutilisation of coal gangue and fly ash as underground backfill materials for surface subsidence control. *Journal of Cleaner Production*, 254, 120113. <https://doi.org/10.1016/j.jclepro.2020.120113>
20. Yang, X., Zhang, Y., Lin, C. (2022). Microstructure analysis and effects of single and mixed activators on setting time and strength of coal gangue-based geopolymers. *Gels*, 8(3). <https://doi.org/10.3390/gels8030195>
21. Yi, C., Ma, H. Q., Chen, H. Y., Wang, J. X., Shi, J. et al. (2018). Preparation and characterization of coal gangue geopolymers. *Construction and Building Materials*, 187, 318–326. <https://doi.org/10.1016/j.conbuildmat.2018.07.220>
22. Yan, C., Ding, Q. J., Xu, J. P., Wang, H. X. (2011). Research on durability performance of novel double solution grouting material with metakaolin. *Advanced Materials Research*, 1270(250–253). <https://doi.org/10.4028/www.scientific.net/AMR.250-253.722>
23. Guo, L., Zhou, M., Wang, X., Li, C., Jia, H. (2022). Preparation of coal gangue-slag-fly ash geopolymer grouting materials. *Construction and Building Materials*, 328, 126997. <https://doi.org/10.1016/j.conbuildmat.2022.126997>
24. Zhao, S., Muhammad, F., Yu, L., Xia, M., Huang, X. et al. (2019). Solidification/stabilization of municipal solid waste incineration fly ash using uncalcined coal gangue-based alkali-activated cementitious materials. *Environmental Science and Pollution Research*, 26(25), 25609–25620. <https://doi.org/10.1007/s11356-019-05832-5>
25. Kleib, J., Aouad, G., Abriak, N. E., Benzerzour, M. (2021). Production of portland cement clinker from French municipal solid waste incineration bottom ash. *Case Studies in Construction Materials*, 15, e00629. <https://doi.org/10.1016/j.cscm.2021.e00629>
26. Luo, H., Cheng, Y., He, D., Yang, E. H. (2019). Review of leaching behavior of municipal solid waste incineration (MSWI) ash. *Science of the Total Environment*, 668, 90–103. <https://doi.org/10.1016/j.scitotenv.2019.03.004>
27. Li, Y., Min, X., Ke, Y., Liu, D., Tang, C. (2019). Preparation of red mud-based geopolymer materials from MSWI fly ash and red mud by mechanical activation. *Waste Management*, 83, 202–208. <https://doi.org/10.1016/j.wasman.2018.11.019>
28. Quina, M. J., Bontempi, E., Bogush, A., Schlumberger, S., Weibel, G. et al. (2018). Technologies for the management of MSW incineration ashes from gas cleaning: New perspectives on recovery of secondary raw materials and circular economy. *Science of the Total Environment*, 635, 526–542. <https://doi.org/10.1016/j.scitotenv.2018.04.150>
29. Joseph, A. M., Snellings, R., Van den Heede, P., Matthys, S., de Belie, N. (2018). The use of municipal solid waste incineration ash in various building materials: A Belgian point of view. *Materials*, 11(1). <https://doi.org/10.3390/ma11010141>
30. Li, X. G., Lv, Y., Ma, B. G., Chen, Q. B., Yin, X. B. et al. (2012). Utilization of municipal solid waste incineration bottom ash in blended cement. *Journal of Cleaner Production*, 32, 96–100. <https://doi.org/10.1016/j.jclepro.2012.03.038>

31. Yang, Z., Ji, R., Liu, L., Wang, X., Zhang, Z. (2018). Recycling of municipal solid waste incineration by-product for cement composites preparation. *Construction and Building Materials*, 162, 794–801. <https://doi.org/10.1016/j.conbuildmat.2017.12.081>
32. Zhang, W., Wang, S., Ran, J., Lin, H., Kang, W. et al. (2022). Research progress on the performance of circulating fluidized bed combustion ash and its utilization in China. *Journal of Building Engineering*, 52, 104350. <https://doi.org/10.1016/j.jobbe.2022.104350>
33. Al Biajawi, M. I., Embong, R., Muthusamy, K., Ismail, N., Obiany, I. I. (2022). Recycled coal bottom ash as sustainable materials for cement replacement in cementitious composites: A review. *Construction and Building Materials*, 338, 127624. <https://doi.org/10.1016/j.conbuildmat.2022.127624>
34. Han, R., Guo, X., Guan, J., Yao, X., Hao, Y. (2022). Activation mechanism of coal gangue and its impact on the properties of geopolymers: A review. *Polymers*, 14(18). <https://doi.org/10.3390/polym14183861>
35. Zhou, C., Liu, G., Yan, Z., Fang, T., Wang, R. (2012). Transformation behavior of mineral composition and trace elements during coal gangue combustion. *Fuel*, 97, 644–650. <https://doi.org/10.1016/j.fuel.2012.02.027>
36. Zhang, Y., Ling, T. C. (2020). Reactivity activation of waste coal gangue and its impact on the properties of cement-based materials—A review. *Construction and Building Materials*, 234, 117424. <https://doi.org/10.1016/j.conbuildmat.2019.117424>
37. Moghadam, M. J., Ajalloeian, R., Hajiannia, A. (2019). Preparation and application of alkali-activated materials based on waste glass and coal gangue: A review. *Construction and Building Materials*, 221, 84–98. <https://doi.org/10.1016/j.conbuildmat.2019.06.071>
38. Chu, S. H., Chen, J. J., Li, L. G., Ng, P. L., Kwan, A. K. H. (2021). Roles of packing density and slurry film thickness in synergistic effects of metakaolin and silica fume. *Powder Technology*, 387, 575–583. <https://doi.org/10.1016/j.powtec.2021.04.029>
39. Provis, J. L., Duxson, P., Lukey, G. C., van Deventer Jannie, S. J. (2005). Statistical thermodynamic model for Si/Al ordering in amorphous aluminosilicates. *Chemistry of Materials*, 17(11), 2976–2986. <https://doi.org/10.1021/cm050219i>
40. Cao, Z., Cao, Y., Dong, H., Zhang, J., Sun, C. (2016). Effect of calcination condition on the microstructure and pozzolanic activity of calcined coal gangue. *International Journal of Mineral Processing*, 146, 23–28. <https://doi.org/10.1016/j.minpro.2015.11.008>
41. Wang, C. L., Ni, W., Zhang, S. Q., Wang, S., Gai, G. S. et al. (2016). Preparation and properties of autoclaved aerated concrete using coal gangue and iron ore tailings. *Construction and Building Materials*, 104, 109–115. <https://doi.org/10.1016/j.conbuildmat.2015.12.041>
42. Zhao, Y., Qiu, J., Ma, Z., Sun, X. (2021). Eco-friendly treatment of coal gangue for its utilization as supplementary cementitious materials. *Journal of Cleaner Production*, 285, 124834. <https://doi.org/10.1016/j.jclepro.2020.124834>
43. Joseph, D., Linwood, S. J. (1985). *Early high-strength mineral polymer*. US, US4509985 A.
44. Wang, K. (2005). Study on grouting material with large amount of coal gangue powder. *New Building Material*, (2), 13–15. <https://doi.org/10.3969/j.issn.1001-702X.2005.02.005>
45. Duxson, P., Provis, J. L., Lukey, G. C., van Deventer Jannie, S. J. (2007). The role of inorganic polymer technology in the development of ‘green concrete’. *Cement and Concrete Research*, 37(12), 1590–1597. <https://doi.org/10.1016/j.cemconres.2007.08.018>